J. Membrane Biol. 165, 183–189 (1998)

The Journal of
Membrane
Biology

Divalent Cation Effects on the Shaker K Channel Suggest a Pentapeptide Sequence as Determinant of Functional Surface Charge Density

F. Elinder, Y. Liu, P. Århem
The Nobel Institute for Neurophysiology, Department of Neuroscience, Karolinska Institutet, S-171 77 Stockholm, Sweden

Received: 12 November 1997/Revised: 1 June 1998

Abstract. The effects of the divalent cations strontium and magnesium on Shaker K channels expressed in *Xenopus* oocytes were investigated with a two-electrode voltage-clamp technique. 20 mM of the divalent cation shifted activation (conductance *vs.* potential), steady-state inactivation and inactivation time constant *vs.* potential curves 10–11 mV along the potential axis. The results were interpreted in terms of the surface charge theory, and the surface charge density was estimated to be $-0.27\ e\ nm^{-2}$. A comparison of primary structure data and experimental data from the present and previous studies suggests that the first five residues on the extracellular loop between transmembrane segment 5 and the pore region constitutes the functional surface charges. The results further suggest that the surface charge density plays an important role in controlling the activation voltage range.

Key words: Shaker K channel — Voltage clamp — *Xenopus* oocytes — Surface charges

Introduction

Surface charges on voltage-gated ion channels have been suggested to play a significant role in channel function (*see* Green & Andersen, 1991; Hille, 1992). The fact that the Debye length in Ringer solution is much shorter than the channel dimensions (9 Å *vs.* 80 × 80 $Å^2$; *see* Hille, 1992; Li et al., 1994) implies that charges located in different extracellular loops contribute differently to the surface charge density sensed by the gating mechanism. In a previous investigation we found a correlation between the experimentally estimated charge densities and the charge of specific extracellular loops of five mammalian K channel clones (Elinder, Madeja & Århem, 1996). The net charge of the loops connecting transmembrane segments S1 and S2 (S1-S2), and segment S5 and the pore region (S5-P) showed positive correlations. However, the total charge of all four extracellular loops also showed a positive correlation. To take the analysis further we have studied two other channels, xKv1.1 and Shaker, the charge profiles of which deviate from those of the other channels studied. In the preceding paper (Elinder & Århem, 1998) we analyzed xKv1.1 and concluded that the functional charges do not belong to the S1-S2 loop. We could not, however, discriminate between the hypothesis that the net charge of the S5-P loop is the major determinant of the functional charge density and the hypothesis that the net charge of all four extracellular loops is the major determinant.

In the present investigation we have analyzed this issue by studying divalent cation induced shifts of gating kinetics for Shaker K channels expressed in *Xenopus* oocytes. As in previous investigations (Elinder et al., 1996; Elinder & Århem, 1998) we chose Sr^{2+} and Mg^{2+} as cations because these have been shown in other preparations to shift gating kinetics less than other divalent cations and been proposed to screen surface charges without binding (Hille et al., 1975; Århem, 1980; Cukierman & Krueger, 1990).

The rationale for the present investigation is indicated in Fig. 1. Regression lines for the relation between experimentally estimated charge densities and the net charge of all four extracellular loops and that of the S5-P loop are plotted for the six Kv channels previously investigated (Elinder et al., 1996; Elinder & Århem, 1997). Assuming that all the extracellular loops contribute equally to the functional charge density of the Shaker channel, the charge density is predicted to be $-0.44\ e\ nm^{-2}$ (net charge is $-7.5\ e$; see arrows and dashed line). Assuming that exclusively the S5-P loop contributes to the functional surface charge density, it is predicted to be

Correspondence to: P. Århem

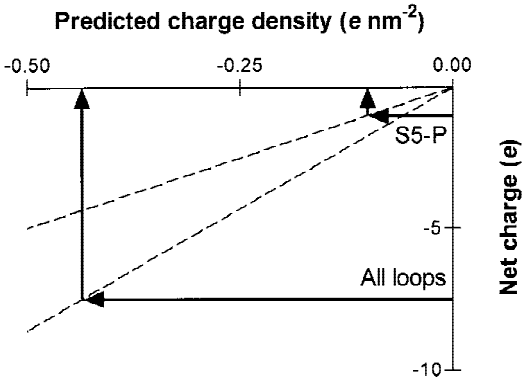

Fig. 1. Predicted charge densities for the Shaker channel based on regression lines (dashed) for the relation between experimentally obtained charge density and net charge of all extracellular loops, and net charge of the S5-P loop for the K channels investigated in Elinder et al. (1996) and Elinder & Århem (1997*b*). The extracellular S5-P loop is defined in the Table. The total sequence is given in Schwarz et al., 1988.

-0.10 *e* nm^{-2} (net charge is -1 *e; see* arrows and dashed line). The relatively large difference between the predicted values should make it possible to evaluate the validity of the two alternatives by experimentally estimating the charge density of the Shaker channel. The results of the investigation showed unexpectedly that the estimated surface charge density was exactly halfway between the two predicted densities. This may seem inconclusive with respect to the predictions above. However, if the S5-P hypothesis is modified by assuming that the putative functional charges only constitute a part of the S5-P loop, the correlation with the experimental estimations is satisfactory.

A preliminary report of these findings has been published (Elinder & Århem, 1997).

Materials and Methods

Molecular Biology

mRNA for ShakerB channels (Schwarz et al., 1988) was prepared as described by Goldin (1992). Templates for transcription were generated by linearizing circular plasmid cDNAs of ShakerB channels (Bluescript KSII) with EcoRI. Transcription reactions were performed with T7 polymerase at 37°C for 1 hr (Stratagene T3 or T7 mCAP mRNA Capping Kit). The resulting mRNA were dissolved in dH_2O and were stored at −70°C until injection. Oocytes of the South African clawed frogs (*Xenopus laevis*) were used as the expression system. Adult female frogs were embedded in ice for 1–2 hr. Stage V and VI oocytes were surgically removed and denuded of overlying follicle cells by agitation for 1–2 hr in 2 mg/ml collagenase type II (Sigma) in Ca^{2+}-free OR-2 buffer (in mM: 82.5 NaCl, 2 KCl, 1 $MgCl_2$, and 5 HEPES, pH 7.5). The in vitro-synthesized mRNA was injected (10–20 ng/cell) using a Nanoject injector (Drummond Scientific, Broomall, PA). The oocytes were maintained at 18–20°C in a modified Barth's solution (in mM: 88 NaCl, 1 KCl, 2.4 $NaHCO_3$, 15 HEPES, 0.33 $Ca(NO_3)_2$, 0.41 $CaCl_2$ and 0.82 $MgSO_4$) supplemented with penicillin (10 μg/ml) and streptomycin (10 μg/ml). The electrophysiological experiments were made 2–8 days after injection of mRNA.

Electrophysiology

The investigations were performed with a two-electrode voltage-clamp technique (CA-1 amplifier, Dagan, Minneapolis, MN). Microelectrodes were made from borosilicate glass and filled with a 2 M KCl solution. The resulting resistance varied between 0.5 and 2.0 MΩ. The amplifier's capacitance and leak compensation was used. The currents were low pass filtered at 2 kHz. All experiments were carried out at room temperature. The control Ringer solution consisted of (in mM): 115 NaCl, 2.5 KCl, 2.0 $CaCl_2$ and 5.0 TRIS buffer adjusted to pH 7.2. Either strontium or magnesium (Sr^{2+}/Mg^{2+}), was added to the Ringer solution. The reason for using these ions is that they are suggested to exert pure screening and no binding (*see* Elinder et al., 1996; Elinder & Århem, 1998).

Data Analysis

The K peak conductance $G_K(V)$ was calculated as

$$G_K(V) = I_K(V)/(V - E_K), \quad (1)$$

where $I_K(V)$ is the K peak current, V is the absolute membrane potential, and E_K is the equilibrium potential, assumed to be −80 mV.

The charge density (σ) was calculated by fitting the experimental data to the Grahame equation (1947):

$$\sigma^2 = 2\varepsilon_r\varepsilon_0 RT\sum_{i=1}^{n} c_i[\exp(-z_i F\psi_0 R^{-1}T^{-1}) - 1], \quad (2)$$

where ε_r is the dielectric constant of the medium, ε_0 is the permittivity of free space, c_i is the bulk concentration and z_i is the valence of the ith ionic species in the extracellular solution, n is the number of ionic species, and ψ_0 is the external membrane surface potential. R, T, and F have their usual thermodynamic significances. The validity of Eq. 2 for the present investigation is discussed in Elinder and Århem (1998).

Results

Effects of Sr^{2+} and Mg^{2+}

Figure 2 shows effects of 20 mM Mg^{2+} on Shaker K currents associated with voltage clamp steps from −60 to +10 mV in steps of 10 mV. The peak current at −20 mV (4th curve from top) is much more reduced (by 90%) than that at +10 mV (top curve; by 35%), indicating a shift of voltage dependent parameters along the potential axis. This is more clearly seen in Fig. 3*A* where control (unfilled circles), 20 mM Mg^{2+} (filled circles), and recovery (unfilled squares) values for the peak conductance are plotted *vs.* potential. A comparison between the dashed curve, which is the control curve (i.e., mean of control and recovery) shifted 13 mV in positive direction, and the 20 mM Mg^{2+} values demonstrates the shift effect. The shift value used (13 mV) is the difference

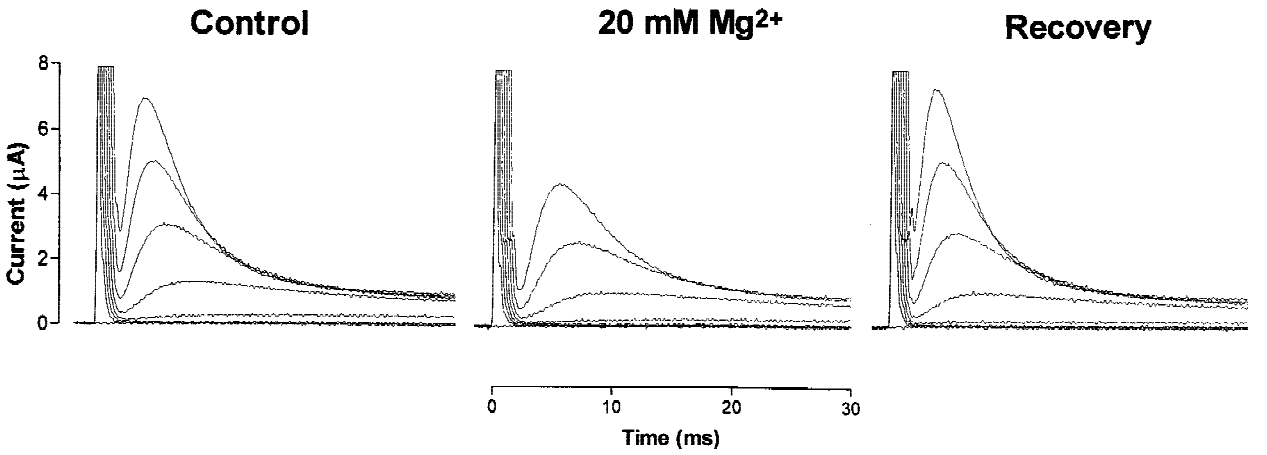

Fig. 2. Effects of 20 mM Mg^{2+} on Shaker K channels. Currents associated with voltage clamp steps from −60 to +10 mV in steps of 10 mV. Holding potential is −60 mV. Low-pass filtered at 2.0 kHz. Capacitive spikes are truncated.

between the control and the 20 mM Mg^{2+} curves at 25% of the maximum value of the control curve (at 10 mV). The 25% level was chosen to minimize the influence of scaling effects on the measured value (*see* Elinder et al., 1996; Elinder & Århem, 1998).

The investigation was based on experiments with various concentrations of both Sr^{2+} and Mg^{2+} on a large number of oocytes. We did not find any systematic difference in shift value between the two cations. The quantitative analysis was based on results from five oocytes, selected for their stable responses and good recovery in control solution. The mean shift (±SEM) of the open probability curve (at the 25% level) caused by 20 mM Sr^{2+}/Mg^{2+} was 10.8 ± 0.7 mV ($n = 5$).

This shift value can be used to estimate the charge density with the Grahame equation (Eq. 2), provided the shift was caused by screening mechanisms and not by binding. As discussed in the previous paper (Elinder & Århem, 1998) this assumption requires that the voltage-dependent parameters of the activation are shifted equally and that the voltage-dependent parameters of the inactivation are shifted equally. Binding often causes the shift of the time constant curves to deviate from that of the steady-state activation or inactivation curves (Hille, 1992; Elinder & Århem, 1994). Assuming further that inactivation is coupled to activation in Shaker channels (as proposed by Zagotta and Aldrich (1990)), pure screening predicts that all voltage-dependent parameters are shifted equally.

The results of the present study was found to be compatible with this pure screening prediction. Figure 3*B* shows the inactivation time constant plotted *vs.* potential for the same cell as in Fig. 3*A*. The dashed line is the control curve shifted by 13 mV, that is the shift of the conductance curve (Fig. 3*A*). As seen, the dashed line closely follows the 20 mM Mg^{2+} curve, supporting the view that the effect mainly is screening induced. The mean shift induced by 20 mM Sr^{2+}/Mg^{2+} and measured at the 7 msec (the current being sufficiently large to be reliably measured but not too fast) was 10.2 ± 1.0 mV ($n = 5$), thus close to the mean shift of the conductance curve described above. Figure 3*C* shows the effects of 20 mM Mg^{2+} on the steady-state inactivation curve. The test step to −10 mV was preceded by 1-sec steps to the potentials indicated. The dashed line indicates the control curve shifted by 13 mV, that is the shift of the conductance curve (Fig. 3*A*). As may be seen it closely follows the 20 mM curve in accordance with the results above.

Figure 3*D* shows the effect of 20 mM Mg^{2+} on the recovery from inactivation. The measurements were made with a conventional double pulse protocol: an activating 20 msec step to +10 mV, a step of variable duration (10–160 msec) to −60, −80, and −100 mV, and a third step to +10 mV. As shown, the tested concentration Mg^{2+} has almost no effect (<10%) on the recovery time constant. However, because of the weak voltage dependence of the recovery, only small effects are expected from a pure screening mechanism. This is in the figure illustrated by the dashed line, indicating the control curve shifted by 13 mV (i.e., the shift of the conductance curve in Fig. 3*A*). In conclusion, the results concerning the shifts of voltage-dependent parameters suggest that the induced shift mainly is caused by a screening mechanism and not by binding to the surface charges, thus validating the use of the Grahame equation (Eq. 2).

Estimation of the Functional Surface Charge Density

Using the mean shift of the conductance curve at 20 mM Sr^{2+}/Mg^{2+} calculated above (10.8 mV) the Grahame

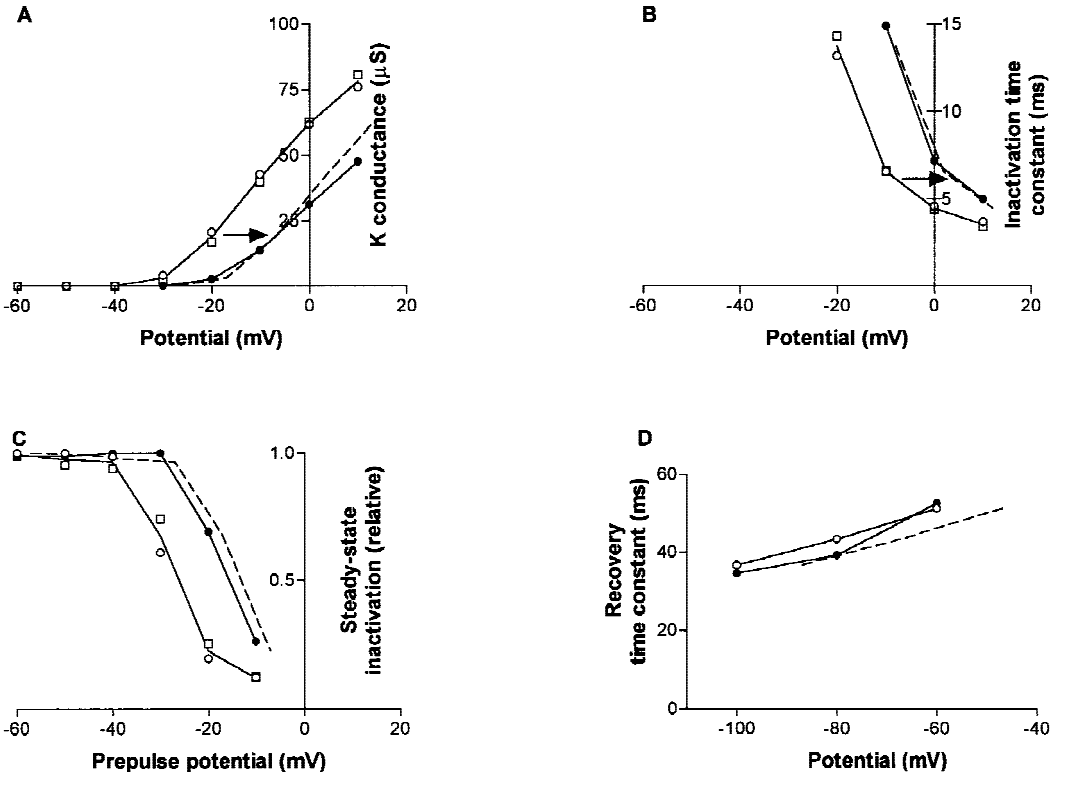

Fig. 3. Shift of voltage-dependent parameters along the potential axis induced by 20 mM Mg^{2+}. (*A*) Peak conductance *vs.* potential in control (open circles), Mg^{2+} (filled circles) and control solution at recovery (open squares). The dashed line is control curve (i.e., average of control and recovery values) shifted 13 mV. (*B*) Inactivation time constant *vs.* potential. Same symbols as in (*A*). (*C*) Steady state inactivation curve. Same symbols as in (*A*). (*D*) Time constant of recovery from inactivation *vs.* potential. Same symbols as in (*A*). Pulse protocols described in the text.

Table 1. Data on S5-Pore sequences and experimental charge density estimations for the seven Kv channels analyzed

Type of channel	S5-P sequence		Net charge of S5-P	Experimental charge density
			(*e*)	(*e* nm^{-2})
Shaker	**E**AGS**E**NSF	F*K*SIP	−1	−0.27
rKv1.1	**EAEE**A**E**S*H*	FSSIP	−3.5	−0.37
xKv1.1	**EAEE**D**E**S*H*	FTSIP	−4.5	−0.45
rKv1.5	**EAD**N*H*GS*H*	FSSIP	−1	−0.17
rKv1.6	**EADDVD**SL	FPSIP	−4	−0.28
rKv2.1	**E***K***DEDD**T*K*	F*K*SIP	−2	−0.17
rKv3.4	**E***R*IGA*R*PS**D**P*R*GN**D***H*T**D**F*K*NIP		+0.5	−0.11

The values for the experimental charge densities are taken from the present study (Shaker), Elinder et al., 1996; rKv1.1, rKv1.5, rKv1.6, rKv2.1 and rKv3.4, and Elinder & Århem, 1998; xKv1.1. Glutamate (**E**) and aspartate (**D**) are assigned a charge of −1, lysine (*K*) and arginine (*R*) +1, and histidine (*H*) +0.5. The sequences are taken from Schwarz et al., 1988; Baumann et al., 1988; Ribera & Nguyen, 1993; Swanson et al., 1990; Grupe et al., 1990; Frech et al., 1989; Schröter et al., 1991.

equation gives a surface charge density of −0.27 *e* nm^{-2}. This value is halfway between the values predicted for the S5-P hypothesis and the total-loop hypothesis (−0.10 *e* nm^{-2} and −0.44 *e* mm^{-2} respectively; *see* Introduction and Fig. 1). This seems to suggest that a combination of the two alternatives is the best explanation. However, because of the short Debye length under the present conditions, a more plausible explanation is that the determinant only comprises part of the S5-P segment. This will be developed in the Discussion.

Discussion

Molecular Identity of the Functional Surface Charges

The present investigation thus did not allow a separation between the two hypotheses concerning the main determinant of the functional charge density with the help of the criteria set out in the Introduction. On the other hand, by plotting the experimentally estimated surface charge densities for the channels in the present (filled circle) and in the preceding investigations (unfilled circles; Elinder et al., 1996; Elinder & Århem, 1998) *vs.* the total net charge of the extracellular loops (Fig. 4*A*) and *vs.* the net charge of the S5-P loop (Fig. 4*B*) some support for the S5-P loop hypothesis, advocated in the preceding investigation of xKv1.1 channels (Elinder & Århem, 1998), can be obtained. The fit is better in the S5-P case than in the all-loops case ($r^2 = 0.87$ *vs.* 0.80).

There are several possible reasons for the discrepancy between the two conclusions. In the absence of a detailed tridimensional picture of the channel the investigation has to be based on a number of more or less realistic assumptions. The channels studied are assumed to have a similar external topology. The Gouy-Chapman theory and the Grahame equation (Eq. 2) are assumed to be applicable. The individual charges of the loops are in practice assumed to contribute equally to the electrostatic field at the voltage sensor. Of these assumptions the last one seems to be the weakest. The Debye length in Ringer solution (*see* Introduction) is sufficiently short to make this assumption questionable. (For the validity of the Gouy-Chapman theory and the Grahame equation, *see* McLaughlin, 1989; Peitzsch et al., 1995; and Elinder & Århem, 1998.) We therefore also considered limited sections of the S5-P loop as putative surface charge determinants. The Table shows the S5-P loop sequences and the experimentally estimated charge densities of the channels used for the correlation analysis (data from the present and the previous investigations; Elinder et al., 1996; Elinder & Århem, 1998). The best correlation was found for the section containing the first five residues (Fig. 4*C*). Furthermore, the correlation was better than that of the full length S5-P loop data ($r^2 = 0.92$ *vs.* 0.87). We also systematically investigated sections of the other loops in a similar way. In no case was a correlation that was better or even close to that of the S5-P pentapeptide sequence found. In conclusion, we suggest that this loop section is the main determinant of the functional surface charge density of Kv channels.

A Physiological Role of Surface Charges?

The present investigation is also of relevance for the idea that the surface charge density is important in regulating the activation range of voltage-gated K channels. In a previous paper (Elinder et al., 1996) we found a clear correlation between the midpoint potential, the potential at which 50% of the channels are activated, and the surface potential in Ringer solution (determined by Eq. 2) for five mammalian K channels. The present investigation of Shaker and xKv1.1 channels (Elinder & Århem, 1998) brings new data to the issue. The surface potential at the voltage sensor for the Shaker K channel in control Ringer solution is −45 mV, which corresponds to a

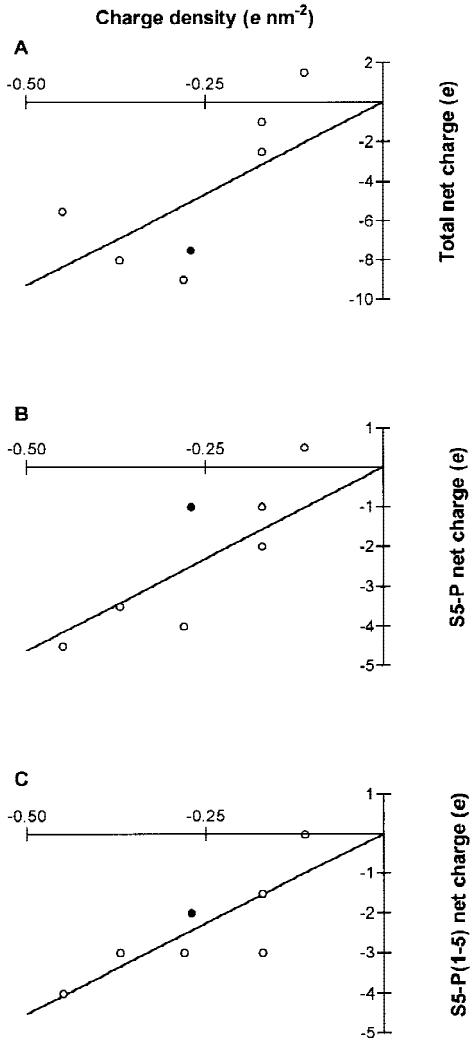

Fig. 4. Relation between the experimentally obtained charge density and the net charge of the four extracellular loops (*A*) of the S5-P loop (*B*) and of the first five amino acids of the S5-P loop (*C*) for the Shaker channel (filled circles) and the Kv channels investigated in Elinder et al. (1996; unfilled circles) and Elinder & Århem (1998; unfilled circles). The amino acid sequences of the investigated S5-P loops are shown in the Table. References to full sequences are listed in the legend. Continuous lines are least-square fitted linear curves through the origin. Slopes are 18.6 nm^2 (*A*), 9.2 nm^2 (*B*), and 9.0 nm^2 (*C*) and r^2 values 0.80 (*A*), 0.87 (*B*) and 0.92 (*C*).

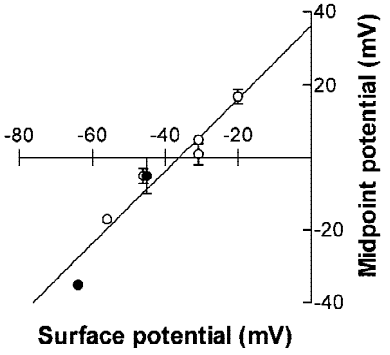

Fig. 5. Relation between midpoint and surface potentials for the channels of the present and previous investigations (Elinder et al., 1996; Elinder & Århem, 1998). The xKv1.1 and Shaker channel denoted by filled circles. The continuous curve is the least-square fit with a fixed slope of 1.0.

charge density of −0.27 e nm^{-2}. The midpoint potential can be estimated to be in the range from −10 to 0 mV (e.g., *see* Fig. 3). The surface potential for the xKv1.1 channel in control Ringer solution was in the previous investigation determined to −64 mV, corresponding to a charge density of −0.45 e nm^{-2} (Elinder & Århem, 1998). In this investigation it was, however, not possible to determine the midpoint potential of the open probability curve because the open probability curve of xKv1.1 channel was not fully separated from that of the other delayed rectifier channel. However, an estimation (*see* Fig. 3*A* in Elinder & Århem, 1998) gives values between −39 and −42 mV. This is in accordance with the results from a patch-clamp study of the xKv1.1 population in *Xenopus* axons by Jonas et al. (1989) where the midpoint value was found to be −35 mV.

Figure 5 shows the relation between the calculated surface potential and the midpoint potential for the Shaker and the xKv1.1 channel in the present and in the preceding investigation (Elinder & Århem, 1998; filled circles) and five Kv channels from a previous study (Elinder et al., 1996; open circles). The continuous line shows a least-square fitted linear curve with a fixed slope of 1.0.

The demonstrated 1:1 relation between surface and midpoint potentials strengthens the idea that the surface charges play an important role in regulating the activation range for the voltage-gated K channels. The y-axis crossing implies that the surface potential in absence of surface charges is +36 mV. This value has implications for the force situation for the gating charges at midpoint potential. Assuming (i) that the internal surface potential is about −15 mV (*see* Hille, 1992; Chandler, Hodgkin & Meves, 1965), and (ii) that the charge *vs.* potential curve, *Q(V),* for the gating charges is located 20 mV in negative direction from the *G(V)* curve (*see* Elinder et al., 1996), the crossover value suggests that the gating charges are half activated at about 0 mV in the absence of internal and external surface charges. This would suggest that nonelectrical forces on the voltage sensor are symmetrical.

Conclusions

In summary, the present investigation suggests that the first five N-terminal residues of the S5-P loop form the main determinant of the functional surface charges in voltage gated K channels. This suggestion entails its own extension. The charges within the limited segment may show individual differences with respect to their influence on the voltage sensor. This will be explored in more detail in a following investigation. Finally, the present investigation strengthens the view that the surface charge density plays a role in regulating the activation range of voltage-gated K channels.

This work was supported by grants from the Swedish Medical Research Council (project nr 6552), Karolinska Institutet, the Swedish Society of Medicine, and Hjärnfonden. We thank Ö. Wrange and U. Björk for assistance with mRNA in vitro transcription and injection of oocytes.

References

Århem, P. 1980. Effects of some heavy metal ions on the ionic currents of myelinated fibres from *Xenopus laevis. J. Physiol.* **306:**219–231

Baumann, A., Grupe, A., Ackermann, A., Pongs, O. 1988. Structure of the voltage-dependent potassium channel is highly conserved from *Drosophila* to vertebrate central nervous systems. *EMBO J.* **7:**2457–2463

Chandler, W.K., Hodgkin, A.L., Meves, H. 1965. The effect of changing the internal solution on sodium inactivation and related phenomena in giant axons. *J. Physiol.* **180:**821–836

Cukierman, S., Krueger, B. K. 1990. Modulation of sodium channel gating by external divalent cation: differential effects on opening and closing rates. *Pfluegers Arch.* **416:**360–367

Elinder, F., Århem, P. 1994. Effects of gadolinium on ion channels in the myelinated axon of *Xenopus laevis:* four sites of action. *Biophys. J.* **67:**71–83

Elinder, F., Århem, P. 1997. Effective surface charges on Shaker K channels are located on the S5-P loop. *Biophys. J.* **72:**A31

Elinder, F., Århem, P. 1998. The functional surface charge density of a fast K channel in the myelinated axon of *Xenopus laevis. J. Membrane Biol.* **165:**175–181

Elinder, F., Madeja, M., Århem, P. 1996. Surface charges of K channels. Effects of strontium on five cloned channels expressed in *Xenopus* oocytes. *J. Gen. Physiol.* **108:**325–332

Frech, G. C., VanDongen, A.M.J., Schuster, G., Brown, A.M., Joho, R.H. 1989. A novel potassium channel with delayed rectifier properties isolated from rat brain by expression cloning. *Nature* **340:**642–645

Goldin, A.L. 1992. Maintenance of *Xenopus laevis* and oocyte injection. *In:* Ion Channels. B. Rudy and L.E. Iversen, editors. pp. 266–279. Academic Press, San Diego, CA

Grahame, D.C. 1947. The electrical double layer and the theory of electrocapillarity. *Chem. Rev.* **41:**441–501

Green, W.N., Andersen, O.S. 1991. Surface charges and ion channel function. *Annu. Rev. Physiol.* **53:**341–359

Grupe, A., Schröter, K.H., Ruppersber, J.P., Stocker, M., Drewes, T., Beckh, S., Pongs, O. 1990. Cloning and expression of a human voltage-gated potassium channel. A novel member of the RCK potassium channel family. *EMBO J.* **9:**1749–1756

Hille, B. 1992. Ionic channels of excitable membranes. pp. 612. Sinauer, Sunderland, MA

Hille, B., Woodhull, A.M., Shapiro, B.I. 1975. Negative surface charge near sodium channels of nerve: divalent ions, monovalent ions and pH. *Phil. Trans. R. Soc. Lond.* **B270:**301–318

Li, M., Unwin, N., Stauffer, K.A., Jan, Y.N., Jan, L.Y. 1994. Images of purified Shaker potassium channels. *Curr. Biol.* **4:**110–115

McLaughlin, S. 1989. The electrostatic properties of membranes. *Ann. Rev. Biophys. Chem.* **18:**113–136

Peitzsch, R.M., Eisenberg, M., Sharp, K.A., McLaughlin, S. 1995. Calculation of the electrostatic potential adjacent to model phospholipid bilayers. *Biophys. J.* **68:**729–738

Ribera, A.B., Nguyen, D.A. 1993. Primary sensory neurons express a Shaker-like potassium channel gene. *J. Neurosci.* **13:**4988–4996

Schröter, K.H., Ruppersberg, J.P., Wunder, F., Rettig, J., Stocker, M., Pongs, O. 1991. Cloning and functional expression of a TEA-sensitive A-type potassium channel from rat brain. *FEBS Lett.* **278:**211–216

Schwarz, T.L., Tempel, B.L., Papazian, D.M., Jan, Y.N., Jan, L.Y. 1988. Multiple potassium-channel components are produced by alternative splicing at the *Shaker* locus in *Drosophila*. *Nature* **331:**137–142

Swanson, R., Marshall, J., Smith, J.S., Williams, J.B., Boyle, M.B., Folander, K., Luneau, C.J., Antanavage, J., Oliva, C., Buhrow, S.A., Bennett, C., Sein, R.B., Kaczmarek, L.K. 1990. Cloning and expression of cDNA and genomic clones encoding three delayed rectifier potassium channels in rat brain. *Neuron* **4:**929–939

Zagotta, W.N., Aldrich, R.W. 1990. Voltage-dependent gating of *Shaker* A-type potassium channels in *Drosophila* muscle. *J. Gen. Physiol.* **95:**29–60